# Ship-in-a-Bottle Synthesis of a Large Guest Occupying Two Y Zeolite Neighbour Supercages: Characterisation and Photocatalytic Activity of the Encapsulated Bipyrylium Ion

Mercedes Alvaro,[a] Esther Carbonell,[a] Antonio Doménech,[b] Vicente Fornés,[a] Hermenegildo García,*[a] and Manoj Narayana[a]

## Introduction

In a series of papers we reported the ship-in-a-bottle synthesis, photochemical properties and photocatalytic applications of 2,4,6-triphenylpyrylium cation (TP$^+$) encapsulated inside the cavities of large pore zeolites Y and Beta.[1, 2] The identity of encapsulated TP$^+$ was then confirmed spectroscopically, particularly by the match of the IR spectra of the encapsulated organic material and that of the tetrafluoroborate solid of TP$^+$ (TPBF$_4$). In addition, the electrochemical response of zeolite Y encapsulated TP$^+$ (TP@Y) consisted of a reversible single reduction process taking place at the same redox potential as that measured for TPBF$_4$ solutions.[3] Encapsulation of TP$^+$ has a dramatic influence on its photophysical and photochemical properties. Thus it was shown that TP@Y emits phosphorescence at room temperature, exhibits a delayed fluorescence emission and has a long-lived (hundreds of µs) triplet excited state.[4] These properties of TP@Y are remarkably different from those exhibited by TP$^+$ in solution, wherein no room temperature phosphorescence or delayed emission are observed. In addition, the lifetime of the excited state in solution is much shorter lived (a few µs). Noteworthy is the fact that, upon illumination of an aqueous suspension of TP@Y, hydroxyl radicals are generated; this capability of TP@Y to generate OH· in water can be exploited in photocatalysis.[5] In this context, it appears to be potentially interesting to explore the photocatalytic properties of related pyrylium dyes. Follow-

ing these previous studies, herein we report the synthesis, characterisation, electrochemical properties and photocatalytic activity of 1,4-bis(3,5-diphenyl-4-pyrylium)phenylene, commonly known as bipyrylium (BTP$^{++}$), encapsulated inside the cavities of zeolite Y. By considering the reported molecular modelling for TP$^+$ inside zeolite Y[6] and the fact that BTP$^{++}$ is an even larger molecule, it is obvious that BTP$^{++}$ can not be accommodated inside a single zeolite Y supercage (13 Å diameter) and would require two neighbour supercages. Therefore the synthesis of BTP$^{++}$ adsorbed in the pore of zeolite Y is particularly challenging. The target of this work is to determine how the special structure of BTP$^{++}$ is reflected in its photocatalytic activity compared to that of TP@Y.

## Results and Discussion

### Synthesis and Characterisation of BTP@Y.

The preparation of bulky BTP$^{++}$ inside zeolites cavities requires a ship-in-a-bottle methodology in which, starting from smaller precursors that can diffuse through the zeolite pores, they undergo a reaction inside the zeolite cages; this leads to a larger reaction product. In the case considered here, the preparation of BTP@Y was accomplished by emulating the synthesis of BTP$^{++}$ in solution, but using acid HY zeolite instead of conventional liquid acids.[7] Thus, as described in the Experimental Section, preparation of BTP$^{++}$ into zeolite Y was carried out by stirring a suspension of dehydrated acidic HY (Si/Al 13) in an isooctane solution of dichalcone and two-fold excess acetophenone at reflux temperature. As the reaction progressed, the HY solid became increasingly bright yellow in colour, which visually indicated that the formation of the pyrylium was taking place. The reaction was allowed to continue for three days to accomplish a high degree of reagent consumption. After the reaction, the solid was submitted to exhaustive solid–liquid extraction to remove unreacted reagents and small by-products.

As expected, molecular modelling at the semiempirical level AM1 clearly shows that BTP$^{++}$ cannot be located in a single cavity of zeolite Y. However, this modelling predicts that, given the size and shape of BTP$^{++}$, it should be possible to accommodate this molecule in two neighbouring supercages. Figure 1 shows a view of the best docking of BTP$^{++}$ inside two Y
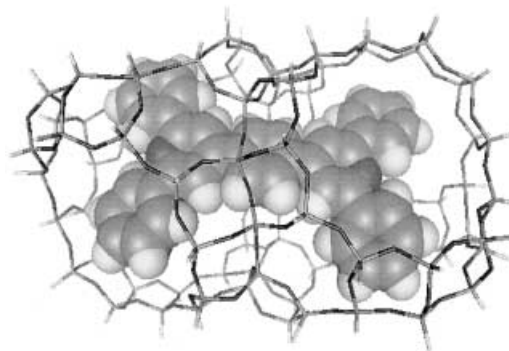


**Figure 1.** Visualisation of the best docking of optimised BTP$^{++}$ within two neighbour supercages of an idealised all-silica Y zeolite.

[a] Prof. H. García, Dr. M. Alvaro, E. Carbonell, Prof. V. Fornés, Dr. M. Narayana
Instituto de Tecnología Química and Departamento de Química
Universidad Politécnica de Valencia
46022 Valencia (Spain)
Fax: (+34) 9 – 6387 – 7807
E-mail: hgarcia@qim.upv.es

[b] Dr. A. Doménech
Department of Analytical Chemistry
University of Valencia
Dr. Moliner 50, 46100 Burjasot, Valencia (Spain)

supercages in which the phenylene ring is crossing through the window connecting the two cages.

The most remarkable structural feature predicted by the molecular modelling is the small deviation of planarity of the pyrylium rings and the connecting phenylene bridge (dihedral angle $8°$). This conformation arises from the compromise between the energy increase (caused by the perturbation of the minimum energy conformation of BTP$^{++}$ in the gas phase) and the minimum unfavourable interaction of BTP$^{++}$ with the zeolite framework. This model, however, neglects the electrostatic interaction between positive pyrylium ion and the negative framework, because it is impossible to locate the exact position of Al atoms in the structure. This rigid configuration is reflected in the absorption spectrum of encapsulated BTP@Y. The electronic spectrum of a series of pyrylium ions substituted at the 2- and/or 4-position of the pyrylium ring has been extensively studied.[8] It has been demonstrated that 2,4,6-triarylsubstituted pyryliums can exhibit two absorption bands in the electronic spectra, which correspond to two independent chromophores defined by the pyrylium core and the aryl ring at the 4-position (shorter wavelength band) and the other absorption due to the 2,6-diarylpyrylium moiety (longer wavelength). The relative intensity of these two absorption bands varies with conformational changes.[8] In our case the diffuse reflectance UV/Vis spectrum shows a shoulder at 380 nm in a more intense band at 330 nm, instead of the two bands observed for the parent TP@Y (380,420 nm). The shoulder at 380 nm most probably corresponds to an unresolved band for the 4-phenylenepyrylium chromophores of BTP@Y. Figure 2 provides a comparison between the optical spectra of BTP@Y and that of an authentic sample of BTP$^{++}$, prepared by reported methods and adsorbed in mesoporous MCM-41. The differences in the spectrum may reflect the rigidity of BTP$^{++}$ inside zeolite that would minimise the relative contribution of the 2,6-diphenylpyrylium chromophore (longer wavelength component in the UV/Vis spectrum of BTP$^{++}$ in solution) due to conformation perturbation. Also the absorption at 330 nm could reflect the presence of some aromatic compounds as impurities (see
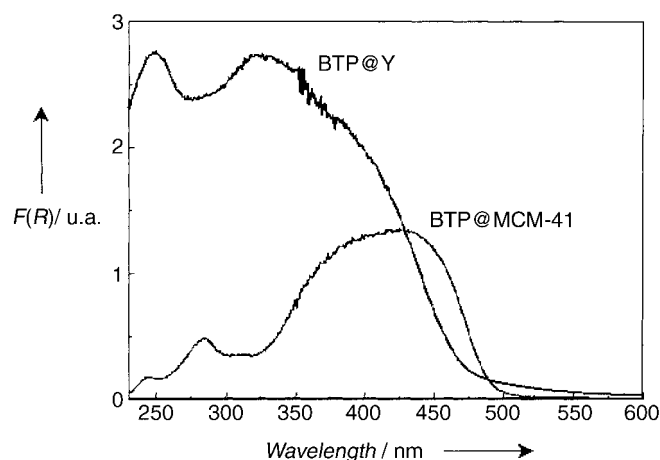
below the discussion of the BTP@Y IR spectrum). Worth noting is the fact that none of the precursors of BTP$^{++}$ exhibits significant absorption above 350 nm.

The resulting BTP@Y was also characterised by IR spectroscopy. The IR spectrum of BTP@Y (Figure 3) also agrees with the structure of bipyrylium and shows as the most characteristic band the one corresponding to the heterocyclic C=O double bond at 1617 cm$^{-1}$, common in pyrylium compounds. It is worth
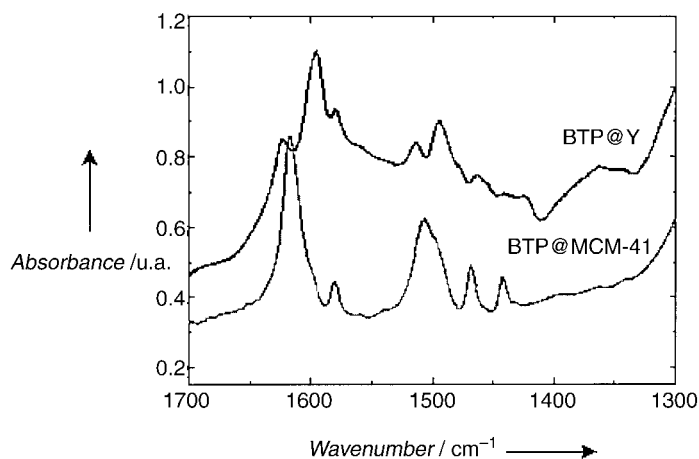
**Figure 3.** IR spectra recorded at room temperature of BTP@Y and an authentic BTP sample adsorbed on MCM-41 (BTP@MCM-41) after outgassing the samples at 200 °C under 10$^{-2}$ Pa for 1 h.

noting that IR bands corresponding to carbonyl groups present in dichalcone and acetophenone (1690 and 1670 cm$^{-1}$) are entirely absent.[9] Taking the IR spectrum as a fingerprint, a comparison between the IR spectra recorded for BTP@Y and an authentic sample of BTP$^{++}$ adsorbed gives an indication of the purity of adsorbed material after the ship-in-a-bottle synthesis. In the case of BTP@Y some extra absorption bands appearing in the spectrum of BTP@Y (particularly that at 1595 cm$^{-1}$) indicates the presence of some impurity in BTP@Y in comparison to the pure BTP@MCM-41. This impurity does not correspond to the starting materials (absence of carbonyl bands), but it can not be removed by solid – liquid extraction. So, most probably these bands are due to bulky entrapped species, also formed in the synthesis of BTP$^{++}$.

The loading of BTP$^{++}$ encapsulated inside the zeolite Y can be estimated from the carbon content measured by combustion chemical analysis. Quantification by combustion chemical analysis requires the absence of any residual solvent (isooctane and dichloromethane), starting reagents or by-product, something that is not completely true here, in view of the IR spectrum. Nevertheless an approximate estimation based on the combustion chemical analysis of BTP@Y can be made. Thus, the solid contains a maximum loading of 4.8% weight of bipyrylium ions, corresponding to an average of one BTP$^{++}$ occupying two cages out of seven. This loading agrees quite well with the initial weight of dichalcone used in the synthesis, indicating that the reaction has occurred to a large extent (including the impurity responsible for the 1595 cm$^{-1}$ IR band). Furthermore, this BTP$^{++}$ loading is similar to that of the TPY@Y samples (5.3% weight,

**Figure 2.** Diffuse reflectance UV/Vis spectrum (plotted as the Kubelka – Munk function of the reflectance F(R)) of BTP@Y and a sample of BTP$^{++}$ adsorbed in mesoporous MCM-41.

one TP$^+$ every three cages) used in this work to compare the photocatalytic activity of BTP@Y.

Additional evidence supporting the successful ship-in-a-bottle synthesis of BTP$^{++}$ was obtained from electrochemical measurements. Upon immersion of a zeolite-modified electrode containing BTP@Y into MeCN or water, well-defined responses were obtained without significant variation of the peak potentials depending on the solvent. As can be seen in Figure 4 for electrodes containing BTP@Y immersed in an aqueous solution (0.10 M NaNO$_3$), cyclic voltammograms (CV) display two apparently one-electron couples with formal electrode potentials (calculated as the half sum of the cathodic and anodic peak potentials) of $-290$ and $-465$ mV versus SCE. No additional peaks were detected upon repetitive potential cycling, the peak current, however, decreased rapidly on successive scans. After prolonged stirring of the BTP@Y solid in water and subsequent filtering, the remaining solution exhibited no electrochemical response, showing that no



Eq. 1

Eq. 2
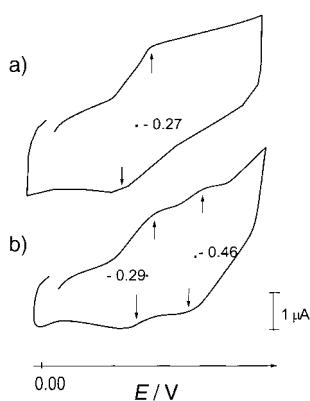


**Figure 4.** Cyclic voltammograms of polymer-film-modified electrodes containing TP@Y (a) or BTP@Y (b), measured in aqueous solutions using 0.1 M NaNO$_3$ as electrolyte. The potential scan rate was 100 mV $\times$ s$^{-1}$.

significant leaching of BTP$^{++}$ from the solid to the aqueous solution takes place under the experimental conditions of the cyclic voltammogram (CV). For the sake of comparison the CV of a zeolite-modified electrode containing TP@Y was also recorded, whereby a single reversible cathodic couple at a formal electrode potential of $-275$ mV was measured (Figure 4a). This reduction potential is similar, although somewhat shifted to lower potentials, to the first reduction peak observed for BTP@Y. The electrochemical response of BTP@Y is characteristic of BTP$^{++}$ without evidence of perturbation due to the impurity.

The two well-defined cathodic peaks recorded for BTP@Y can be attributed to the two successive one-electron processes indicated in Equations (1) and (2), which correspond to the stepwise reduction of the two pyrylium rings of BTP$^{++}$. The reduction of the first ring considerably diminishes the electron-acceptor ability of the second one, which consequently appears at more negative potentials.
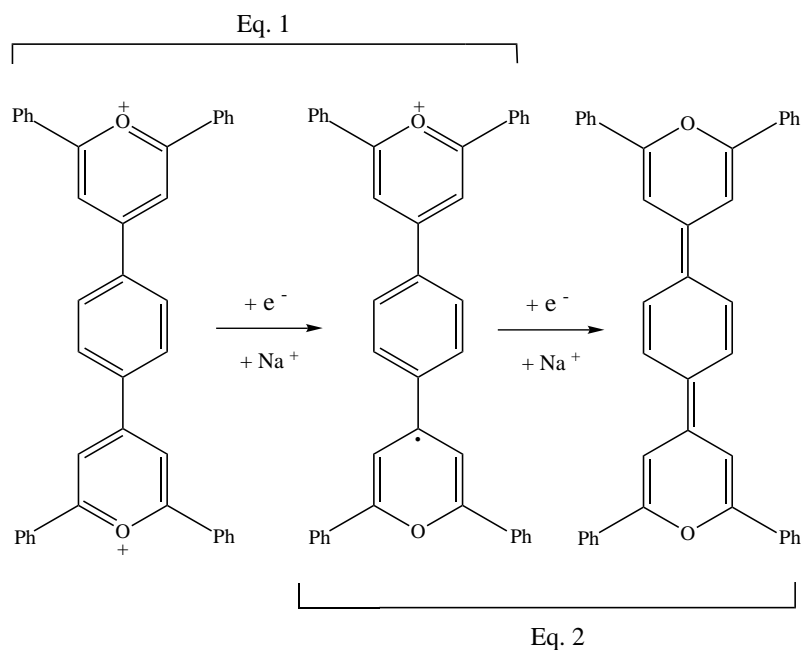
The current intensity of the electrochemical measurement of BTP@Y is lowered using Et$_4$NClO$_4$ or Bu$_4$NPF$_6$ as a supporting electrolyte instead of NaNO$_3$. Although Et$_4$N$^+$ cations can enter the zeolite pores,[10] the Bu$_4$N$^+$ cation is essentially size-excluded from the zeolite Y cage and pore system.[11] Thus, the decrease of electroactivity observed using Et$_4$NClO$_4$ and Bu$_4$NPF$_6$ electrolytes (about a factor of one fifth) can be attributed to the intrazeolitic location of BTP$^{++}$. Since the electrochemical response requires the diffusion of an accompanying electrolyte concomitantly to the electron transfer process [see Equations (1) and (2)] during the electrochemical scan, only the population of the most external electroactive guests is active. Nevertheless, the influence of the size of cationic electrolyte (Na$^+$, Et$_4$N$^+$ or Bu$_4$N$^+$) indicates that some shallow penetration into the zeolite particle occurs.

## Photocatalytic Activity

The main potential application of BTP@Y would be its use as a photocatalyst to effect the degradation of pollutants in aqueous solutions. In previous work we studied the photocatalytic activity of parent TP@Y for the degradation and mineralisation of pesticides.[12–14] For TP@Y we have provided evidence of the stability of TP$^+$ in water and in support of the intermediacy of the hydroxyl radical.[5] Herein we want to compare the photocatalytic efficiency of the novel BTP@Y with that of TP@Y. To do this, we chose the degradation of phenol in water, a reaction that has been proposed as a test to measure the photocatalytic activity of different photocatalysts, particularly TiO$_2$.[15]

When studying the photocatalytic activity of a photocatalyst, two are the major parameters to be considered. The first parameter is the initial activity estimated from the slope of the temporal phenol disappearance profile, which is measured at zero time. The second parameter is the degradation percentage at long reaction times. Figure 5 shows the temporal profile for
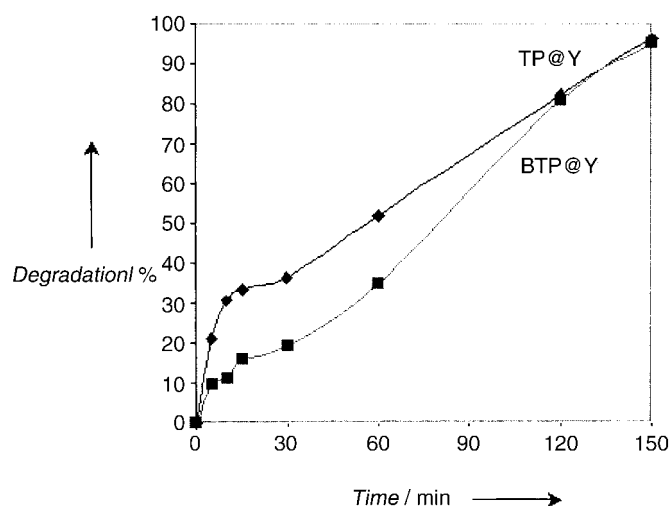
**Figure 5.** *Photocatalytic activity for phenol degradation (40 ppm) in aqueous solution (20 mL) using TP@Y or BTP@Y as photocatalysts (100 mg) through Pyrex.*

phenol degradation using TP@Y and BTP@Y as the photocatalyst. From these curves it can be seen that the initial activity for TP@Y is 3.5% min$^{-1}$, that is, higher than that of BTP@Y (2.0% min$^{-1}$).

Given that the loading of TP$^+$ and BTP$^{++}$ is similar for both photocatalyst, the higher initial activity of TP@Y with respect to BTP@Y could be due to one or a combination of the following reasons: i) stronger electron-acceptor ability of encapsulated TP$^+$ ($E_{red} = -0.270$ V vs. SCE) than BTP$^{++}$ ($E_{red} = -0.290$ V vs. SCE); ii) the presence of impurities in BTP@Y that quench the excited state of BTP$^{++}$ and impedes diffusion of reagent and products, and iii) more favourable diffusion of phenol through the zeolite pores for TP$^+$ as compared to BTP$^{++}$, due to the larger molecular size. It has to be considered that for BTP$^{++}$ two neighbour supercages are occupied, while in the case of TP$^+$ it can be considered that all the cations are isolated and accessible through any of four cavity windows. Regardless of the lower initial activity, what is remarkable is that the final photocatalytic activity measured at long reaction times is the same for both solids. In the other words, although BTP@Y is a less active photocatalyst the percentage of phenol degradation at long irradiation times for BTP@Y reaches the same value as TP@Y.

## Conclusion

We have described a highly demanding ship-in-a-bottle synthesis in which a big guest requires not one but two neighbour cavities to be accommodated. Spectroscopic and electrochemical data support the formation of encapsulated BTP$^{++}$ although some adventitious material seems to be present on the solid. The resulting BTP@Y solid exhibits a notable photocatalytic activity for the degradation of phenol, although no advantages in terms of higher initial activity or higher degree of degradation have been observed for BTP@Y over the parent TP@Y.

## Experimental Section

Preparation and characterisation of the TP@Y and BTP@Y:

TP@Y was prepared from a commercial NaY (PQ CBV 100) following the reported procedure.[6] To prepare BTP@Y, a solution of dichalcone [1,4-bis(3-phenyl-3-oxo-1-propene)phenylene] (50 mg) and acetophenone (50 mg) in isooctane (25 mL) was stirred magnetically in the presence of thermally dehydrated (500 °C) HY zeolite (PQ CBV 720, 1 g) at reflux temperature for seven days. Dichalcone was in turn obtained by Claisen–Schmidt condensation of two equivalents of acetophenone (9.84 g) with one equivalent of terephthaldehyde (Aldrich, 5 g) in ethanol (25 mL) containing NaOH (3.28 g) at room temperature. During the ship-in-a-bottle synthesis the solid became increasingly yellow. After the reaction, the raw BTP@Y solid was submitted to exhaustive solid-liquid extraction using Soxhlet apparatus and dichloromethane as the solvent. BTP@Y was characterised by combustion chemical analysis (Fisons CHNS analyser) and spectroscopic techniques. Diffuse reflectance UV/Vis spectra were recorded in a Cary 5G spectrophotometer with an integrated sphere using BaSO$_4$ as standard. FTIR spectra were recorded in a Nicolet 710 spectrophotometer using sealed greaseless CaF$_2$ cells. The wafers (10 mg) were prepared by pressing the powders at (200–300) MPa. The IR spectra were recorded at room temperature after outgassing the samples at 200 °C under 10$^{-2}$ Pa for one hour.

Molecular modeling BTP@Y was performed with the Hyperchem 6.02 program starting with optimised BTP$^{++}$ geometry at the semiempirical level AM1, and considering the Faujasite as a rigid matrix with the atoms located at the crystallographic positions. An idealised all-silica cluster devoid of framework aluminium and charge-balancing cations was considered. This cluster is neutral and does not contain separate charges. The docking of BTP$^{++}$ inside the two faujasite cavities was performed with molecular mechanics calculations. Visualisation of the model was drawn using the Viewer Lab. Pro program.

Zeolite-modified electrodes were prepared, as previously described,[16] by transferring a few microlitres (typically 50 µL) of a dispersion of the zeolite (10 mg) in acetone (5 mL) to the surface of the freshly polished glassy carbon electrode and allowing the suspension to dry in air. After the electrode dried, one drop of a solution of an acrylic resin (1%) in acetone was added and the modified electrode was air-dried. Commercially available Paraloid B72, an ethyl acrylate (70%)-methyl acrylate (30%) co-polymer, was selected for polymer-film electrode preparation because of its mechanical stability and ability to form porous films able to adhere the zeolite microparticles to the electrode surface.[3, 17] This facilitates a direct contact between the zeolite particles and the substrate electrode, which is a crucial aspect for studying the electrochemistry of zeolite-associated species.[18–20] The films examined contained 0.2–1.5 mg × cm$^{-2}$ of the dry zeolite.

Cyclic voltammograms were performed with a BAS CV50W equipment. A standard three-electrode arrangement was used with a platinum auxiliary electrode and a saturated calomel reference electrode (SCE) in a thermostated cell. As basal electrodes, glassy carbon (BAS MF 2012, geometrical area 0.071 cm$^2$) and platinum (BAS MF 2013, geometrical area 0.017 cm$^2$) electrodes were used. Experiments were conducted in aqueous media using LiNO$_3$, NaNO$_3$ and KNO$_3$ (all Panreac reagents), or acetonitrile using Et$_4$NClO$_4$ and Bu$_4$NPF$_6$ (Aldrich) as supporting electrolytes. All electrochemical measurements were performed in well-deaerated solutions under an atmosphere of argon.

Photocatalytic activity: Tests were carried out using aqueous solutions of phenol (Aldrich 40 ppm) in MilliQ water (20 mL). The corresponding photocatalyst (100 mg) was added to this solution,

and the suspension stirred magnetically. Irradiations were carried out using a 125 W medium pressure Hg lamp cooled by water, through Pyrex. The test tubes were placed surrounding the lamp well and independent tubes were used for each data point. At the required reaction time, the corresponding tube was taken and the suspension was centrifuged. To recover adsorbed phenol and products, the solid was sonicated in ultrasound bath (25 W power) with additional 3 mL MilliQ water for 10 min. After this time the suspension was centrifuged and the extracted liquor was combined with the photolysed solution. The phenol present in the combined aqueous solution was quantified by quantitative HPLC using a reverse-phase column and a mixture of $CH_3CN$/water (36:64) as eluent. The concentration of phenol was determined by integration of the chromatographic peak using a diode away detector UV/Vis and 280 nm as the monitoring wavelength.

[1] J. C. Scaiano, H. García, *Acc. Chem. Res.* **1999**, *32*, 783.

[2] H. García, H. D. Roth, *Chem. Rev.* **2003**, *103*, 3547.

[3] A. Domenech, M. T. Domenech-Carbo, H. García, M. S. Galletero, *Chem. Commun.* **1999**, 2173.

[4] M. L. Cano, F. L. Cozens, H. García, V. Marti, J. C. Scaiano, *J. Phys. Chem.* **1996**, *100*, 18 152.

[5] A. Sanjuán, M. Alvaro, G. Aguirre, H. García, J. C. Scaiano, *J. Am. Chem. Soc.* **1998**, *120*, 7351.

[6] A. Corma, V. Fornés, H. García, M. A. Miranda, J. Primo, M. J. Sabater, *J. Am. Chem. Soc.* **1994**, *116*, 2276.

[7] N. Manoj, R. Ajit Kumar, K. R. Gopidas, *J. Photochem. Photobiol., A* **1997**, *109*, 109.

[8] M. A. Miranda, H. García, *Chem. Rev.* **1994**, *94*, 1063.

[9] C. J. Pouchert, *The Aldrich Library of Infrared spectra*, 2nd ed., Aldrich Chemical Company, Inc., **1975**.

[10] G. T. Kerr, *Zeolites* **1983**, *3*, 295.

[11] H. A. Gemborys, B. R. Shaw, *J. Electroanal. Chem.* **1986**, *208*, 95.

[12] A. Sanjuán, G. Aguirre, M. Alvaro, H. García, *Water Res.* **1999**, *34*, 320.

[13] A. Sanjuán, G. Aguirre, M. Alvaro, H. García, *Appl. Catal: B* **1998**, *15*, 247.

[14] A. Sanjuán, G. Aguirre, M. Alvaro, H. García, J. C. Scaiano, *Appl. Catal. B* **2000**, *25*, 257.

[15] T. Zhang, T. Oyama, A. Aoshima, H. Hidaka, J. Zhao, N. Serpone, *J. Photochem. Photobio., A* **2001**, *140*, 163.

[16] A. Domenech, P. Formentin, H. García, M. J. Sabater, *J. Phys. Chem. B* **2002**, *106*, 574.

[17] A. Domenech, H. García, M. T. Domenech-Carbo, M. S. Galletero, *Anal. Chem.* **2002**, *74*, 562.

[18] C. A. Bessel, D. R. Rolison, *J. Phys. Chem. B* **1997**, *101*, 1148.

[19] G. Calzaferri, M. Lanz, J.-W. Li, *J. Chem. Soc. Chem. Commun.* **1995**, 1313.

[20] J.-W. Li, K. Pfanner, G. Calzaferri, *J. Phys. Chem.* **1995**, *99*, 12 368.

# Photocatalytic and Photoelectrochemical Properties of Nitrogen-Doped Titanium Dioxide

Shanmugasundaram Sakthivel and Horst Kisch*[a]

*Dedicated to Professor Günter O. Schenck on the occasion of his 90th birthday.*

## 1. Introduction

The application of titanium dioxide as a mutual photocatalyst for solar purification of air and water[1a] is based on its semiconductor properties. In the direct semiconductor-photocatalysis mechanism[1b] absorption of UV light by titania generates surface-trapped electron-hole pairs, which undergo the interfacial processes of oxygen reduction and substrate oxidation. The resulting superoxide and substrate radical cation initiate a multistep reaction that leads to partial or complete mineralization. Since titania absorbs only 2 – 3 % of solar light, many attempts were made to improve its poor solar-energy-conversion efficiency. Whereas light absorption can be easily shifted to the larger, visible part of the solar spectrum by doping with metal ions, this is not in general true for the photocatalytic activity.

During our work on titania modified with platinum(IV)chloride[2] we observed that the hydrolysis of titanyl sulfate or titanium tetrachloride by ammonia afforded a slightly yellow material that photocatalyzed the degradation of 4-chlorophenol with visible light ($\lambda \geq 455$ nm). This result is in accord with the earlier observation that calcination of ammonium chloride containing titania at 400 °C gave a yellow material that was active in the photooxidation of carbon monoxide and ethane by visible light.[3a] In three other publications, modified titania materials were recently reported to be also active in the visible light. One was concerned with a V(IV)-doped monolayer of $TiO_2$ prepared by chemical vapor deposition onto porous borosilicate glass. This monolayer catalyzed photooxidation of gaseous ethanol with light of $\lambda = 396 – 450$ nm, as indicated by solid-state NMR spectroscopic analysis.[3b] Another reported on metal ion-implanted titania that was active in 2-propanol degradation ($\lambda \geq 450$ nm).[3c] The third paper dealt with a nitrogen-doped titania that was obtained upon heating anatase powder at 600 °C in an

[a] Prof. Dr. H. Kisch, Dr. S. Sakthivel
Institut für Anorganische Chemie
Universität Erlangen-Nürnberg
Egerlandstr.1, 91058 Erlangen (Germany)
Fax: (+49) 9131-852-7363
E-mail: kisch@chemie.uni-erlangen.de